Journal of Applied Polymer Science

Blast furnace slags as functional fillers on rheological, thermal, and mechanical behavior of thermoplastics

Abdelhamid Mostafa,[1] Stephan Laske,[2] Gernot Pacher,[1] Clemens Holzer,[2] Helmut Flachberger,[3] Elke Krischey,[3] Bertram Fritz[4]

[1]Polymer Competence Center Leoben GmbH (PCCL), Leoben, Austria
[2]Chair of Polymer Processing, Montanuniversitaet Leoben, Leoben, Austria
[3]Chair of Mineral Processing, Montanuniversitaet Leoben, Leoben, Austria
[4]voestalpine Stahl, Linz, Austria
Correspondence to: S. Laske (E-mail: stephan.laske@tugraz.at)

ABSTRACT: Blast furnace slags (BFS) is a secondary byproduct of iron industry, which has a combination of acidic and basic oxides and show a complex, multiphase structure. If appropriately tailored, BFS could be an effective functional filler, improving the property profile of thermoplastics such as polypropylene (PP) and polystyrene (PS). As a raw material, the proposed filler may introduce both economic and ecological advantages, as it is considered an inexpensive secondary product rather than a natural resource. The current study aims at investigating the effect of incorporating BFS as a micro-sized filler on the rheological, thermal, and mechanical behavior of PP and PS. BFS types in this study are air-cooled, crystalline, and amorphous, grounded types. Both types are ground into 71, 40, and 20 μm batches and introduced in 10, 20, and 30 weight fractions via melt kneading. Mixtures are then formed into 4-mm and 2-mm thick plates via compression molding. Slight increase in rheological factors is observed with increasing filler loading. BFS hinders the crystallization of PP, resulting in slight increase of crystallization temperatures (T_c) and lowering of crystallization enthalpy (ΔH_c). No significant effect of filler on transition temperatures (T_g) is reported. Mechanically, BFS increases the tensile modulus of PP, but decreases its strength. For PS formulations, a modest toughening effect is observed by slag filler. © 2015 Wiley Periodicals, Inc. J. Appl. Polym. Sci. **2016**, *133*, 43021.

KEYWORDS: composites; extrusion; polyolefins

Received 25 August 2015; accepted 8 October 2015
DOI: 10.1002/app.43021

INTRODUCTION

Global interest has been directed toward using mineral particulate fillers for thermoplastic composites throughout the last few decades. It was shown that incorporation of mineral fillers in thermoplastic matrices has been a smart choice for reducing the material costs and improving functional properties like strength, stiffness, wear resistance, and flame retardance. In fact, the choice of mineral filler can significantly affect the overall composite behavior. That is, filler composition, size, type, morphology, and surface chemistry are all key factors that influence the performance of the filler within the thermoplastic host matrix.[1–3] Conventional fillers such as calcium carbonate, talc, mica, alumina, and silica have been successfully incorporated into many thermoplastic matrices because of their low cost compared to polymer carriers. Employment of such fillers was widely reported to ameliorate many functional properties in many polymeric systems, and thermoplastics are no exception.[4–10] However, such fillers are all nonrenewable natural resources. They are extracted from mines or quarries that are susceptible to depletion, which is a major environmental concern.[11] Therefore, it is instructive to study other material candidates that could compete as fillers in polymer industry. Such candidates should be abundant, economic, nontoxic, and environmentally benign. Blast furnace slags (BFS), the multi-oxide material floating above iron in blast furnaces, could potentially meet such requirements.

BFS are the byproducts of iron industry. They are much less dense that iron; hence, they float above the metal and are easily extracted. Compared to many conventional fillers, BFS are "manufactured" byproducts rather than natural resources. They are cheap and abundant as one ton of iron produces nearly 0.2–0.4 tons of BFS.[12] BFS are composed of four main oxides: calcium oxide (CaO), silicon oxide (SiO_2), aluminum oxide (Al_2O_3), and magnesium oxide (MgO) beside other secondary oxides and elements such as manganese oxide (MnO) and sulfur (S).[13] BFS are currently used in road building or as a

Table I. Composition and Properties of BFS[22]

Constituent	Amount	Property	Value
CaO	35–42		
SiO_2	33–38	Particle density (g/cm^3)	2.4
Al_2O_3	10–15	Compressive strength (N/mm^2)	100
MgO	7–12	Impact value (%)	27
FeO	≤1.0	Resistance to polishing	50
MnO	≤1.0	Water absorption (%)	2
S_{total}	1–1.5	Resistance to freeze/thaw (%)	<0.5
Cr_2O_3	≤0.1		

mixture with clinker and Portland cement in concrete as well as other important applications in civil, marine, and agriculture industries.[14–16] Despite many calls to stop disposing slags due to their benefits, still considerable amount of slags are being landfilled. That imposes serious environmental concerns, as landfilling of slags is a noneconomic, unsustainable solution.[11,17–19]

In fact, investigation of BFS behavior as a filler for thermoplastic matrices has been almost lacking in literature. In addition, almost there are no systematic studies to investigate such application of BFS. One of the modest attempts to utilize BFS in polymeric systems is the incorporation of BFS with/without short glass fibers in polypropylene (PP) matrix, as reported by Padhi's team.[20,21] It was concluded that incorporation of BFS was an important key factor in improving the wear resistance of PP. The current study, hence, aims to provide a novel, systematic approach to assess the effect of two types of BFS as functional fillers in two thermoplastic polymers: semi-crystalline PP and amorphous polystyrene (PS). Rheological, thermal, and mechanical behavior of the compounds are addressed.

EXPERIMENTAL

Material

Borealis PP BB412E grade and Styrolution PS 116N/L were used as base polymers. BB412E has a density of 900 kg m^{-3} and a melt flow rate of 1.3 g 10 min^{-1}. It was provided by the company Borealis, Austria. PS 116N/L was provided by company Styrolution, Germany. It has a melt volume rate of 23 cm^3 10 min^{-1} and a density of 1040 kg m^{-3}. Granulated (GBS) and air-cooled (ACBS) are two types of BFS. They were supplied by the company voestalpine Stahl GmbH, Linz, Austria in the form of 1–3 mm aggregates. Composition and properties of BFS are illustrated in Table I.[22] Grinding of GBS and ACBS types into respective mesh sizes was performed at the Chair of Mineral Processing, Montanuniversitaet Leoben, Austria.

Particle Size Distribution Analyses

Particle size distribution analyses of milled slags were successfully accomplished at voestalpine Stahl GmbH Company using CILAS 920 Particle Size analyzer using laser diffraction technique. The test was done in wet mode using isopropyl alcohol as the dispersing agent.

Composite Preparation

Kneading at 175°C (PP) and 155°C (PS) was performed via Haake Polylab System 3000P laboratory kneader, Thermo Fischer Scientific, Waltham, USA. Kneading time of 10 min (from the time the filler was added) and constant rotor rotation of 60 rpm were maintained for all conditions. Neat polymer samples were also produced for referencing. Loadings of 10, 20, and 30 wt % were investigated. At least three replicate plates with thickness of 2 mm (for rheology and thermal properties) and 4 mm (for tensile properties) were produced for each adjustment via (Collin 200 PV, Dr. Collin, Ebersberg, Germany) hydraulic vacuum press machine. PP and PS formulations are shown in Table II.

Rheological Investigation

Rheological behavior was analyzed via double plate Physica MCR 501 rheometer (Anton Paar, Graz, Austria). Plate geometry and gap used were 25 mm and 1 mm, respectively. The 2-mm thick samples were subjected to nitrogen atmosphere for degradation prevention. Two testing modes were used for investigation: (1) dynamic strain sweep to identify viscoelastic region and (2) dynamic frequency sweep to measure complex viscosity, storage and loss moduli. The frequency range of 0.1–500 rad s^{-1} was maintained for all samples, and all measurements were insured to be within the viscoelastic range.

Thermal Investigation

Thermal behavior was tested via a 4000 differential scanning calorimeter (Perkin Elmer, USA). Experiments were conducted using about 10 mg samples, sealed in aluminum cups. Heating and cooling rates were fixed at 10°K min^{-1}. Samples were subjected to one cooling and two heating cycles. Degree of

Table II. Experimental Parameters (Reproduced from ANTEC 2015 Proceedings[24] with Permission from Publisher)

Sample	Filler particle size (μm)	Matrix weight fraction (wt %)	Filler weight fraction (wt %) ACBS	GBS
	Neat polymer	100	0	0
71	10ACBS	90	10	
	10GBS	90		10
	20ACBS	80	20	
	20GBS	80		20
	30ACBS	70	30	
	30GBS	70		30
40	10ACBS	90	10	
	10GBS	90		10
	20ACBS	80	20	
	20GBS	80		20
	30ACBS	70	30	
	30GBS	70		30
20	10ACBS	90	10	
	10GBS	90		10
	20ACBS	80	20	
	20GBS	80		20
	30ACBS	70	30	
	30GBS	70		30

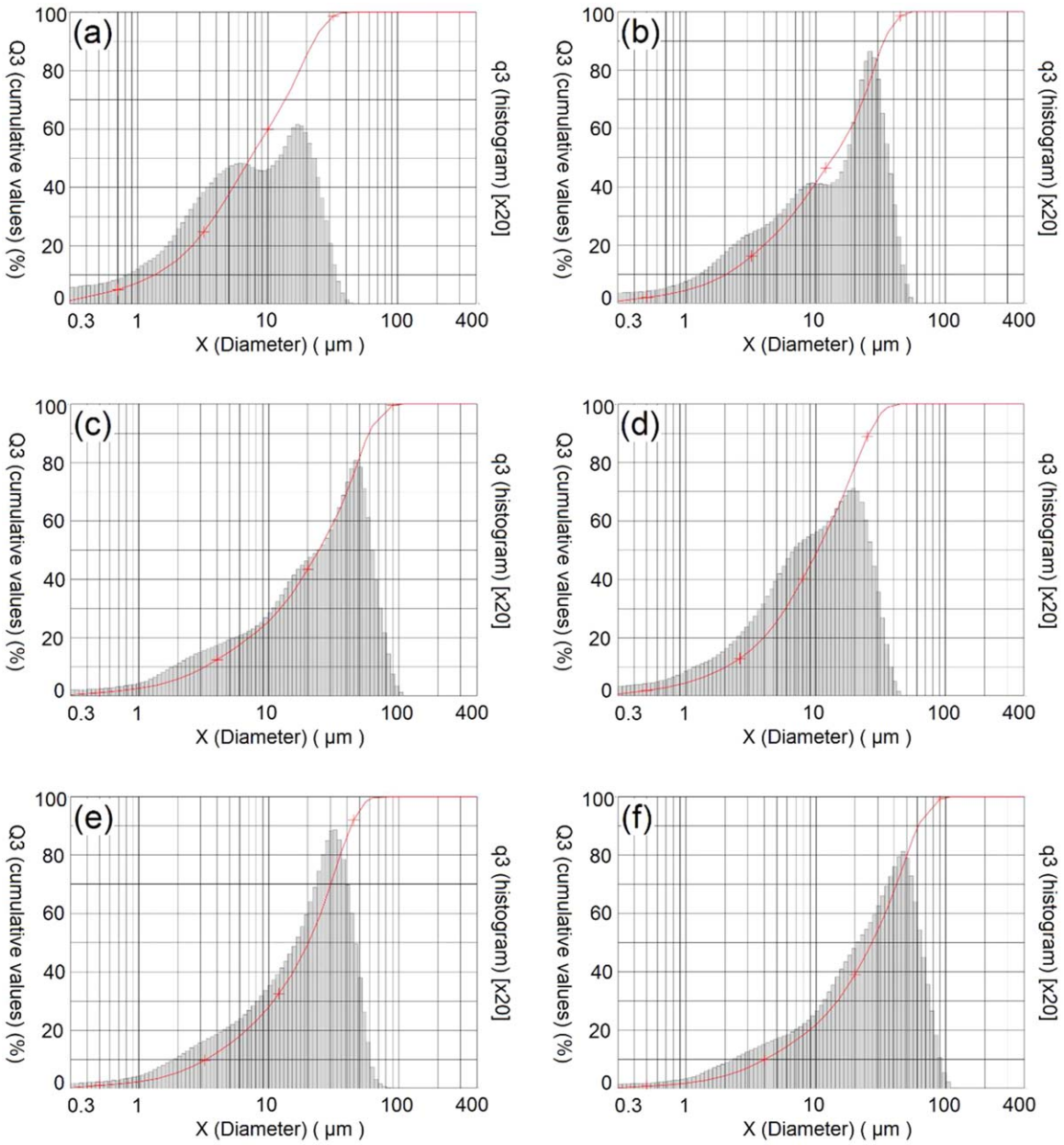

Figure 1. Cumulative particle size distribution for ACBS 0–20, 0–40, 0–71 (a–c) and GBS 0–20, 0–40, 0–71 (d–f). [Color figure can be viewed in the online issue, which is available at wileyonlinelibrary.com.]

crystallinity, ΔX_c, is defined as the ratio between sample melting enthalpy and the melting enthalpy of 100% crystalline PP (was taken as 209 J/g) according to Marinelli *et al.*[23]

Mechanical Investigation

Tensile behavior was investigated via Zwick/Roell testing station (Zwick and Co.KG, Ulm, Germany) according to the standard ISO 527-1. Constant rate of 50 mm min^{-1} was maintained for all conditions, and testing was accomplished in room temperature. Samples were milled out of 4 mm pressed plates to standard dog-bone shape, and data from at least three replicates were averaged per condition. Data were evaluated using testXpert II software.

RESULTS AND DISCUSSION

Particle Size Distribution

Figure 1 shows the particle size distribution for all slag size groups. Median D50 particle sizes can be easily identified from the graphs, which correspond to the cumulative value of 50%. For instance, D50 particle sizes of about 7 and 25 μm is determined from cumulative distribution of ACBS 0–20 and ACBS 0–71 categories, as shown in Figure 1 (a,c). The distribution graphs show that most of the particles lie below or equal to the size upper limit of interest in each condition.

Rheological Findings

The effect of particle size and amount on rheology of PP was reported elsewhere.[24] Rheological performance of PS-slag

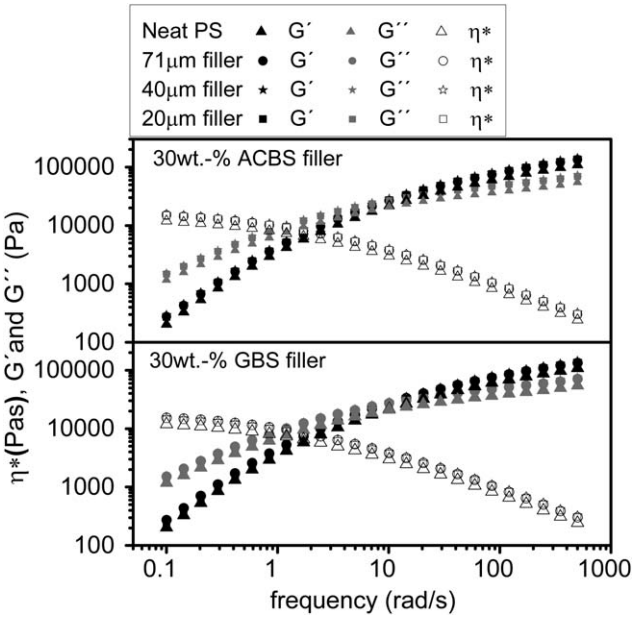

Figure 2. Complex viscosity η^*, loss and storage moduli, G′ and G″, versus frequency exemplary for PS formulations with 30 wt % filler.[24]

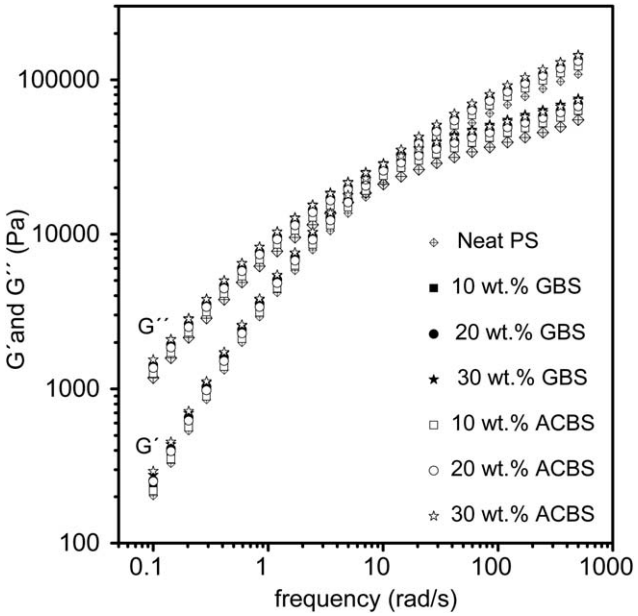

Figure 4. Storage and loss moduli, G′ and G″, versus frequency exemplary for PS formulations with 40 μm filler.

formulations is shown in Figures 2 and 4. As expected, non-Newtonian shear thinning behavior was recorded, where shear viscosity decreases as frequency increases. Storage and loss moduli, however, increased with frequency. Shear viscosity increased with particle amount due to restriction of molecular chains by filler particles. Similar to what was previously reported for PP,[24] there was no significant increase in shear viscosity for PS resulted from increasing of filler size and/or content. That comes in agreement with other studies of similar systems such as talc-filled and mica-filled PP.[25] It was reported that sharp increase was observed only above 30 and 40 wt % of 10 μm talc and 12 μm mica fillers, respectively. It was believed that appearance of agglomerates after critical weight fraction was the reason behind such increase in viscosity. Modest increase in complex viscosity was also reported for another system of PS filled with up to 30 wt % of 1 μm calcium carbonate.[5] Such findings could interpret the current situation for PP and PS/BFS systems, where the critical filler content was not reached.

Crossover points represent the intersections of storage and loss modulus curves. They are fundamental in illustration viscous behavior of the material with frequency change. Effect of slag filler loading and type on cross over frequency and modulus results for PP was previously reported.[24] As shown in Figure 5, crossover frequency and modulus components for PS were plotted as a function of filler content for 40-μm filler formulations for PS. Similar to PP observations, it was noticed that crossover frequencies for PS were almost independent of filler type and/or content. That indicates almost no change in relaxation time of

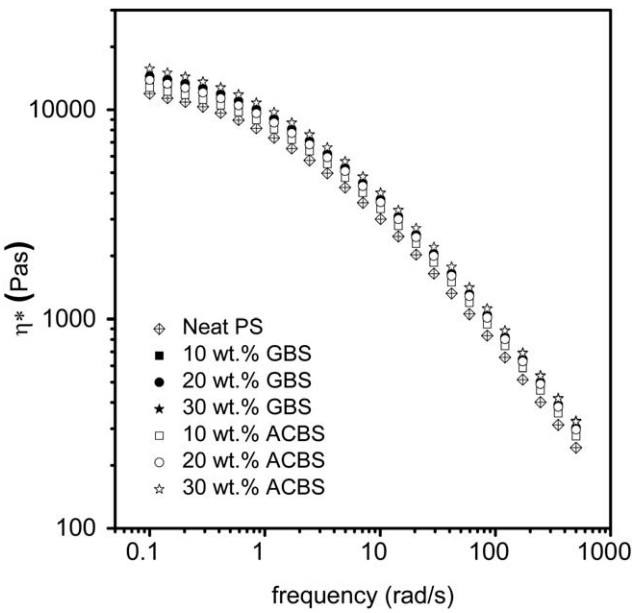

Figure 3. Complex viscosities versus frequency exemplary for PS formulations with 40 μm filler.[24]

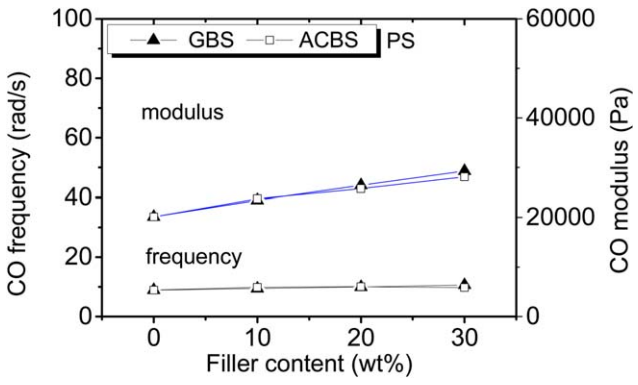

Figure 5. Crossover (CO) frequencies and moduli versus filler content exemplary for PS formulations with 40 μm filler.[24] [Color figure can be viewed in the online issue, which is available at wileyonlinelibrary.com.]

Table III. DSC Results of PP Composite Formulations (Reproduced from ANTEC 2015 Proceedings[24] With Permission from Publisher)

Condition	T_c (°C)		ΔH_c (J/g)		T_m (°C)		ΔH_m (J/g)		ΔX_c (%)	
Neat PP	118.9	±0.56	91.6	±13.40	167.6	±0.69	92.5	±11.18	44.7	±0.69
S1PP10A	118.9	±0.23	74.4	±1.55	167.3	±0.23	75.5	±1.61	36.2	±0.23
S1PP10G	119.2	±0.07	78.6	±2.16	167.2	±0.09	77.4	±2.82	37.0	±0.09
S1PP20A	118.8	±0.16	67.4	±5.20	167.0	±0.13	67.9	±5.60	32.6	±0.13
S1PP20G	119.1	±0.35	73.9	±8.08	167.5	±0.58	73.6	±7.40	35.2	±0.58
S1PP30A	118.9	±0.12	63.4	±1.93	166.7	±0.11	63.3	±0.81	30.3	±0.11
S1PP30G	120.3	±0.21	60.9	±1.32	167.0	±0.21	62.0	±1.07	29.3	±0.21
S2PP10A	116.9	±0.74	82.2	±1.39	168.7	±1.07	82.3	±2.47	39.4	±1.07
S2PP10G	118.4	±0.23	79.5	±0.42	168.1	±0.47	79.8	±1.13	37.9	±0.47
S2PP20A	118.3	±0.39	68.5	±5.03	167.7	±0.37	70.4	±3.90	33.2	±0.37
S2PP20G	118.0	±0.06	71.9	±8.75	168.5	±0.16	72.2	±8.37	34.2	±0.16
S2PP30A	119.0	±0.50	70.4	±0.63	167.4	±0.59	67.8	±2.40	33.5	±0.59
S2PP30G	118.1	±0.30	72.8	±7.62	168.2	±0.40	72.6	±7.15	34.8	±0.40
S3PP10A	118.6	±0.42	85.9	±6.56	168.1	±0.67	86.4	±5.69	41.2	±0.67
S3PP10G	118.4	±0.01	76.0	±5.44	168.4	±0.12	76.3	±5.11	36.1	±0.12
S3PP20A	118.6	±0.62	76.5	±14.30	168.2	±0.77	79.9	±10.20	37.9	±0.77
S3PP20G	118.2	±0.01	76.0	±5.10	168.5	±0.11	78.2	±7.67	36.7	±0.11
S3PP30A	119.7	±0.23	71.5	±1.20	167.4	±0.35	71.1	±1.68	33.2	±0.35
S3PP30G	118.8	±0.14	74.7	±0.13	167.9	±0.36	74.4	±0.47	35.3	±0.36

PP and PS composites. Crossover modulus, on the other hand, increased with increasing filler content, but not much deviation was recorded in comparing both filler types. It is suggested that such increase is probably due to restriction of chain movements imposed by filler particles, which could lead to a more elastic and solid-like behavior.[26]

Thermal Findings

PP Formulations. Thermal behavior of slag filler for PP formulations were formerly reported and the results are tabulated in Table III.[24] T_c and ΔH_c decreased with increasing filler loading, reflecting the tendency of the filler particle to resist the formation of crystallized regions. That explained the decrease of crystallinity with increased loading.[24]

PS Formulations. As shown in Table IV, T_g for the different formulations were not significantly affected by size, type, or content of slag microfiller, and very slight change in values compared to neat polymer were noticed. This came in agreement with other studies,[27–29] where the behavior of microfillers such as calcium carbonate, glass beads, and CdS within high-density polyethylene, PP, poly(lactic acid), and PS and PS–copolymer matrices was investigated. The authors observed that T_g values were not much influenced by 1–5 μm fillers for up to 40 wt % loading. On the other hand, dramatic increase in T_g toward higher values was reported for nanoparticles with a mean diameter of 5 nm.[30] It is believed that the high surface to bulk ratio of nanofillers is one of the reasons for such significant altering in behavior, as it facilitates much stronger interaction of fillers with the matrix. Effective filler treatment could also provide significant enhancement of matrix–filler chemical and mechanical bonding.[31,32]

Mechanical Findings

Tensile properties of PP and PS formulations as compared to neat polymers are shown in Tables V and VI. For PP, it was observed that all formulations still exhibited necking prior to

Table IV. DSC Results of PS Composite Formulations (Reproduced from ANTEC 2015 Conference Proceedings[24] With Permission from Publisher)

Condition	T_g (°C)	
Neat PS	88.88	±0.46
S1PS10A	87.79	±0.96
S1PS10G	87.66	±0.88
S1PS20A	88.82	±0.11
S1PS20G	88.51	±0.33
S1PS30A	88.38	±0.35
S1PS30G	88.31	±0.21
S2PS10A	87.19	±0.24
S2PS10G	87.36	±0.17
S2PS20A	86.83	±0.82
S2PS20G	87.00	±0.25
S2PS30A	87.19	±0.67
S2PS30G	86.66	±0.52
S3PS10A	86.60	±0.28
S3PS10G	86.86	±0.01
S3PS20A	87.44	±0.02
S3PS20G	86.27	±0.40
S3PS30A	86.83	±0.30
S3PS30G	87.58	±0.34

Table V. Tensile Properties for PP formulations

Sample	Filler particle size (μm)	Modulus (MPa)	Yield strength (MPa)	Ultimate strength (MPa)	Ultimate strain (%)	Strength at break (MPa)	Strain at break (%)
Neat PP		1485.7	7.89	24.30	4.60	18.68	115.50
10ACBS	71	1605.54	8.21	23.06	4.10	18.13	66.60
10GBS		1609.02	8.09	22.90	4.50	17.51	99.65
20ACBS		1793.67	9.19	21.76	3.85	17.31	60.45
20GBS		1742.29	9.09	20.25	3.90	16.69	68.65
30ACBS		1893.14	9.76	20.93	3.75	18.25	42.90
30GBS		1779.22	8.73	19.39	3.85	16.88	37.30
10ACBS	40	1428.64	7.98	22.43	4.45	15.96	71.35
10GBS		1516.90	8.68	22.44	4.25	17.05	71.55
20ACBS		1669.15	9.44	21.14	3.73	16.02	59.23
20GBS		1684.18	8.55	19.84	3.85	15.52	60.10
30ACBS		1804.46	9.90	20.40	3.65	16.63	47.25
30GBS		1818.09	9.31	19.18	3.85	15.72	50.20
10ACBS	20	1529.43	8.95	22.28	4.45	18.29	192.50
10GBS		1407.43	7.22	20.10	4.63	16.73	122.30
20ACBS		1678.17	8.78	21.88	4.05	17.26	75.45
20GBS		1673.10	9.25	21.32	4.00	17.66	124.00
30ACBS		1820.36	9.38	20.87	3.60	16.79	88.87
30GBS		1803.41	9.27	19.93	3.83	16.45	126.73

Table VI. Tensile Properties for PS formulations

Sample	Filler particle size (μm)	Modulus (MPa)	Yield strength (MPa)	Ultimate strength (MPa)	Ultimate strain (%)	Strength at break (MPa)	Strain at break (%)
Neat PS		3434.28	17.61	36.99	1.70	36.26	1.70
10ACBS	71	3711.48	18.52	34.24	1.67	32.68	1.93
10GBS		3759.92	19.68	35.33	1.63	34.08	1.93
20ACBS		3886.27	18.68	32.05	1.53	31.41	1.73
20GBS		3984.48	18.33	31.22	1.55	30.98	1.70
30ACBS		4230.84	18.31	30.08	1.53	29.27	1.70
30GBS		4186.60	18.58	29.17	1.43	28.83	1.43
10ACBS	40	3668.03	19.79	33.02	1.40	32.79	1.45
10GBS		3911.38	19.87	35.66	1.60	35.18	1.70
20ACBS		4096.48	20.10	33.01	1.45	32.05	1.45
20GBS		4141.54	19.43	33.37	1.60	32.29	1.75
30ACBS		4549.00	20.56	31.88	1.40	31.06	1.50
30GBS		4398.94	18.71	30.59	1.55	29.88	1.70
10ACBS	20	3652.43	19.32	35.61	1.75	34.15	1.75
10GBS		3607.82	18.68	34.40	1.85	32.62	1.85
20ACBS		3796.29	19.28	33.29	1.55	31.95	1.80
20GBS		3875.52	18.99	32.32	1.50	31.10	1.90
30ACBS		4341.25	20.74	31.83	1.40	30.37	1.55
30GBS		4271.07	19.39	30.61	1.45	29.39	1.80

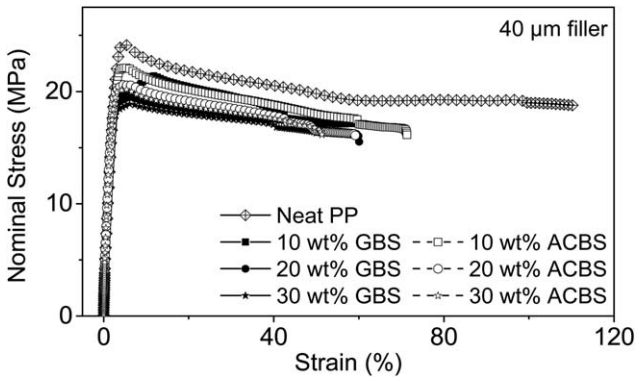

Figure 6. Nominal stress–strain curves of PP formulations with 40 μm filler.

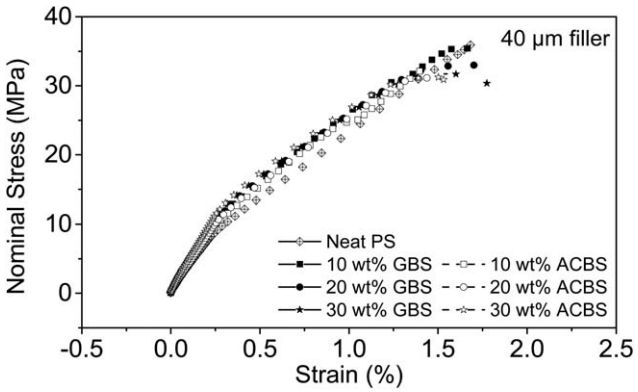

Figure 7. Modulus versus filler content of PP formulations with 40 μm filler.

fracture, indicating that ductility was not much sacrificed even with 30 wt % loading level. Increasing filler loading lead to an increase in modulus and yield strength. However, ultimate strength as well as strength-at-break decreased. It was also observed that ultimate strength values were less than that of neat polymer, and further decreased with increasing filler loading. Increasing of modulus and/or yield strength values with increasing filler loading (micro/nano) is a typical behavior for many reinforced polymer composites. Ultimate strength and strength-at-break, on the other hand, decreased with increasing filler loading. It is believed that such decrease is a result of poor adhesion between the filler and the polymer as no filler treatment was introduced. In addition, large filler particles could have acted as stress concentration sites, causing rapid failure at lower stress levels.[32] Accordingly, ultimate strain range of the composites were much narrower than that of neat polymer. Such findings were expected as filler sizes from submicron up to only few microns were reported to yield satisfying mechanical properties in different microsized mineral-filled thermoplastic systems, as reported by Nurdina *et al.*,[3] Luo *et al.*,[33] and Selvin *et al.*[34] Though such range exists within the current compounds, as previously illustrated via particle size distribution curves, its enhancing effect is believed to be counteracted by: (1) the effect of coarser, i.e., >10 μm, particles of slag and (2) the poor compatibility and debonding of slag particles from polymer matrices. Tensile and modulus values for PP compounds are shown in Table VI and are graphically illustrated in Figures 6 and 7. It was observed that 71-μm filler group showed highest modulus while 20-μm filler group showed highest strain-at-break values. Yield and ultimate strength values, however, were not significantly affected by filler size. It was also noticed that strength and modulus values show little improvement with ACBS filler.

For PS formulations, as shown in Figures 8 and 9, modulus and yield strength increased, while ultimate strength decreased with increasing filler loading. For 71-μm and 20-μm filler groups, formulations with ACBS fillers showed higher modulus, higher yield, ultimate strength, and strength-at-break values compared to GBS formulations. An opposite trend, however, was shown for 40-μm filler group. It is important to notice that strain-at-break values were always greater than ultimate strain values for most composite formulations, suggesting that incorporation of slag microfiller, although untreated, introduced a modest toughening effect on PS. That came in agreement with some reported PS systems.[34,35]

CONCLUSIONS

Incorporation of BFS filler sizes up to 71-μm and weight fractions up to 30 wt % resulted in modest increase in shear viscosity. With respect to slag-filled compounds, modest increase recorded for viscosity values may appear as a positive indicator

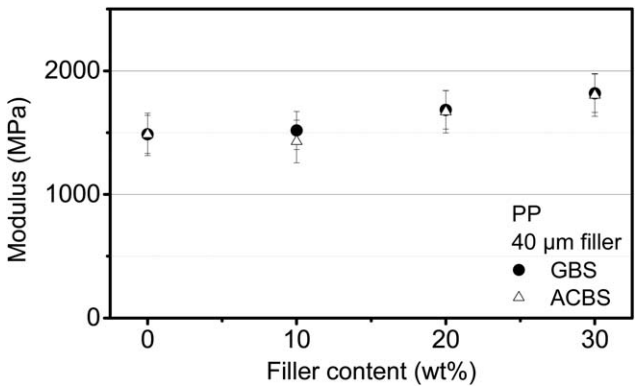

Figure 8. Nominal stress–strain curves of PS formulations with 40 μm-filler.

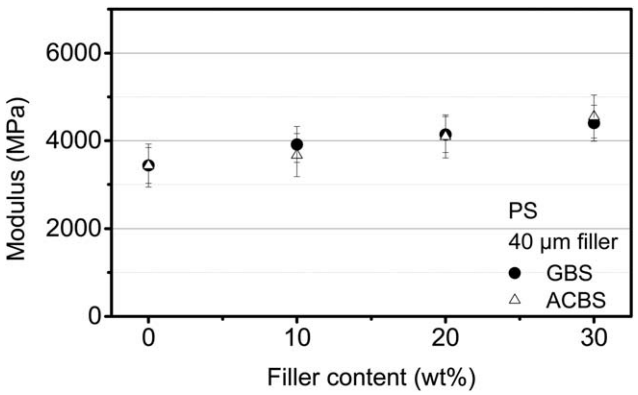

Figure 9. Modulus versus filler content of PS formulations with 40 μm filler.

toward easier processability. Thermal properties were slightly affected through changing of crystallization and glass transition temperatures as coarse fillers are believed to resist chain motion rather than acting as nucleation initiators. For PP, stiffness increased proportionally with filler amount and was almost independent of filler type. However, strength and elongation levels of filled compounds deteriorated, as compared with neat polymer. Different behavior was recorded for PS compounds where both strength and elongation schemes were almost unaffected by slag filler, while stiffness increased proportionally with filler loading.

In general, it is concluded that incorporation of untreated BFS provided promising results in terms of rheological behavior and stiffness of the filled compounds. Improving of filler/polymer computability may greatly enhance or at least stabilize strength and/or elongation levels. In addition, low price of filler material may introduce high potential for modification and tailor-made pre-processing. That is, a novel sophisticated filler capable of introducing attractive enhancements to the property profile of thermoplastics could be hence produced. This research is considered an initial, yet believed crucial, step toward more understanding of slag functionalities in thermoplastics. More research, however, is mandatory to reveal such functionalities.

ACKNOWLEDGMENTS

Current study was achieved at Polymer Competence Center Leoben GmbH (PCCL, Austria) within the framework of the Austrian Research Promotion Agency (FFG). Invaluable contributions toward the fulfillment of this research were provided by company voestalpine Stahl GmbH, Chair of Polymer processing and Chair of Mineral Processing, Montanuniversitaet Leoben. PCCL is funded by the Austrian Government and the State Governments of Styria and Upper Austria.

REFERENCES

1. Jancar, J.; Fekete, E.; Hornsby, P. R.; Jancar, J.; Pukánszky, B. Rothon, R. N., Eds. Mineral Fillers in Thermoplastics I; Springer: Berlin, Heidelberg, 27 May **1999**; p 139.
2. Lozano, T.; Lafleur, P. G.; Grmela, M.; Thibodeau, C. *Polym. Eng. Sci.* **2014**, *44*, 880.
3. Nurdina, A. K.; Mariatti, M.; Samayamutthirian, P. *J. Vinyl Addit. Technol.* **2014**, *15*, 20.
4. Bartczak, Z.; Argon, A.; Cohen, R.; Weinberg, M. *Polymer (Guildf)* **2015**, *40*, 2347.
5. Lou, J.; Harinath, V. *J. Mater. Process. Technol.* **2014**, *152*, 185.
6. Zha, L.; Fang, Z. *Polym. Compos.* **2014**, 1258.
7. Sheril, R. V.; Mariatti, M.; Samayamutthirian, P. *J. Vinyl Addit. Technol.* **2014**, *20*, 160.
8. Zuiderduin, W. C.; Westzaan, C.; Huétink, J.; Gaymans, R. *Polymer (Guildf)* **2014**, *44*, 261.
9. Velasco, J. I.; Saja, J. A.; Martinez, A. B. *J. Appl. Polym. Sci. 61*, 125.
10. Pustak, A.; Pucić, I.; Denac, M.; Švab, I.; Pohleven, J.; Musil, V.; Šmit, I. *J. Appl. Polym. Sci.* **2014**, *128*, 3099.
11. Drew, L. J.; Langer, W. H.; Sachs, J. S. *Nat. Resour. Res.* **2015**, *11*, 19.
12. Nesbit, C. C. Environmentally Conscious Materials and Chemicals Processing—Myer Kutz; John Wiley & Sons, Inc., **2007**.
13. Das, B.; Prakash, S.; Reddy, P. S. R.; Misra, V. N. *Resour. Conserv. Recycl.* **2014**, *50*, 40.
14. Mihok, L.; Demeter, P.; Baricova, K.; Seilerova, K. *Metallurgija* **2006**, *45*, 163.
15. Asmatulaev, B. A.; Asmatulaev, R. B.; Abdrasulova, A. S.; Levintov, B. L.; Vitushchenko, M. F.; Stolyarskiiv, O. A. *Steel Transl.* **2015**, *37*, 722.
16. National Slag Association. http://www.nationalslag.org/blast-furnace-slag; Accessed **2015**.
17. Francis, A. A. *J. Eur. Ceram. Soc.* **2015**, *24*, 2819.
18. Mansfeldt, T.; Dohrmann, R. *Environ. Sci. Technol.* **2015**, *38*, 5977.
19. Bayless, E. R.; Schulz, M. S. *Environ. Geol.* **2015**, *45*, 252.
20. Padhi, P. K.; Satapathy, A. *Int. Polym. Process.* **2014**, *29*, 233.
21. Padhi, P. K.; Satapathy, A.; Nakka, A. M. *J. Thermoplast. Compos. Mater.* **2014**, *28*, 656.
22. Euroslag. http://www.euroslag.com/; Accessed **2015**.
23. Marinelli, A. L.; Bretas, R. E. S. *J. Appl. Polym. Sci.* **2014**, *87*, 916.
24. Mostafa, A.; Laske, S.; Holzer, C.; Flachberger, H.; Krischey, E.; and Buergler, T.
25. Jahani, Y. *J. Vinyl Addit. Technol.* **2014**, *16*, 70.
26. Mezger, T. G. The Rheology Handbook: For Users of Rotational and Oscillatory Rheometers; **2006**.
27. Gorna, K.; Hund, M.; Vučak, M.; Gröhn, F.; Wegner, G. *Mater. Sci. Eng. A* **2014**, *477*, 217.
28. Bergeret, A.; Alberola, N. *Polymer (Guildf)*. **2014**, *37*, 2759.
29. Kuljanin, J.; Vučković, M.; Čomor, M. I.; Bibić, N.; Djoković, V.; Nedeljković, J. M. *Eur. Polym. J.* **2014**, *38*, 1659.
30. Djoković, V.; Nedeljković, J. M. *Macromol. Rapid Commun.* **2014**, *21*, 994.
31. Samsudin, M. S. F.; Ishak, Z. A. M.; Jikan, S. S.; Ariff, Z. M.; Ariffin, A. *J. Appl. Polym. Sci.* **2015**, *102*, 5421.
32. Bartczak, Z. *J. Macromol. Sci. Part B* **2014**, *41*, 1205.
33. Luo, F.; Chen, L.; Ning, N.; Wang, K.; Chen, F.; Fu, Q. *J. Appl. Polym. Sci.* **2015**, *125*, E348.
34. Selvin, T. P.; Kuruvilla, J.; Sabu, T. *Mater. Lett.* **2014**, *58*, 281.
35. Flores-Hernandez, M.; Gonzalez, I. R.; Lomeli-Ramirez, M.; Fuentes-Talavera, F.; Silva-Guzman, J.; Cerpa-Gallegos, M.; Garcia-Enriquez, S. *J. Compos. Mater.* **2014**, *48*, 209.